

The dynamics of recycled acetylcholine receptors at the neuromuscular junction in vivo

Emile G. Bruneau and Mohammed Akaaboune*

At the peripheral neuromuscular junction (NMJ), a significant number of nicotinic acetylcholine receptors (AChRs) recycle back into the postsynaptic membrane after internalization to intermingle with not-yet-internalized 'pre-existing' AChRs. However, the way in which these receptor pools are maintained and regulated at the NMJ in living animals remains unknown. Here, we demonstrate that recycled receptors in functional synapses are removed approximately four times faster than pre-existing receptors, and that most removed recycled receptors are replaced by new recycled ones. In denervated NMJs, the recycling of AChRs is significantly depressed and their removal rate increased, whereas direct muscle stimulation prevents their loss. Furthermore, we show that protein tyrosine phosphatase inhibitors cause the selective accumulation of recycled AChRs in the peri-synaptic membrane without affecting the pre-existing AChR pool. The inhibition of serine/threonine phosphatases, however, has no effect on AChR recycling. These data show that recycled receptors are remarkably dynamic, and suggest a potential role for tyrosine dephosphorylation in the insertion and maintenance of recycled AChRs at the postsynaptic membrane. These findings may provide insights into long-term recycling processes at less accessible synapses in the central nervous system in vivo.

KEY WORDS: Recycling, Receptor dynamics, Half-life, Phosphorylation, Synaptic activity

INTRODUCTION

At central synapses, recycling of postsynaptic receptors plays a crucial role in synaptic plasticity. For example, during long-term potentiation, synaptic strength is enhanced by an increased recruitment of recycled α -amino-5-hydroxy-3-methyl-4-isoxazole propionic acid (AMPA) receptors from intracellular endosomal compartments to the postsynaptic membrane (Contractor and Heinemann, 2002; Ehlers, 2000; Lee et al., 2004; Luscher et al., 1999; Park et al., 2004). At the peripheral neuromuscular junction (NMJ), it was long assumed that acetylcholine receptors (AChRs) remain stable in the postsynaptic membrane until they are internalized and degraded in the lysosomes (Gardner and Fambrough, 1979). In this scheme, insertion of newly synthesized receptors would be responsible for maintaining AChR density in the postsynaptic membrane over time. Recent work from our laboratory has shown, however, that a significant number of internalized AChRs are not degraded, but instead return back into the postsynaptic membrane where they intermingle with AChRs that have not yet been internalized and retain their initial fluorescent tag (referred to hereafter as 'pre-existing' AChRs) (Bruneau et al., 2005). However, the way these AChR pools are maintained and regulated remains to be determined.

The involvement of phosphorylation in the trafficking, insertion and maintenance of ionotropic receptors in central synapses has been extensively studied, and has been found to play an important role in regulating synaptic changes that lead to either long-term potentiation or long-term depression (Carroll et al., 1999; Ehlers, 2000; Hayashi et al., 2000; Lee et al., 2000; Malinow and Malenka,

2002). At the NMJ, a large body of work demonstrates that phosphatases are involved in AChR anchoring and clustering in vivo and in vitro (Grady et al., 2003; Haganir et al., 1984; Li et al., 2004; Mei and Si, 1995; Wallace, 1994; Wallace et al., 1991); however, the role of phosphorylation/dephosphorylation events in AChR recycling at the NMJ in vivo has not previously been investigated.

In order to investigate the dynamics of recycled and pre-existing AChR pools, and the potential role of phosphorylation/dephosphorylation in AChR recycling, we monitored recycled and pre-existing AChRs using a sequential labeling method that we had previously used to selectively identify recycled and pre-existing receptor pools in the postsynaptic membrane (Bruneau et al., 2005). Here, we report that recycled receptors are removed more quickly than pre-existing receptors from the same postsynaptic membrane of functional synapses, and demonstrate that denervation decreases the insertion of recycled AChRs and increases their removal rate. In addition, we found that tyrosine phosphatase inhibitors, but not serine/threonine phosphatase inhibitors, cause the aberrant peri-synaptic accumulation of recycled AChRs.

MATERIALS AND METHODS

Live animal imaging

All animal usage followed methods approved by the University of Michigan Committee on the Use and Care of Animals. Adult female mice (20-27 g; NSA, Harlan Sprague Dawley, Indianapolis, IN) were anesthetized with an intraperitoneal injection of ketamine and xylazine (KX; 87 mg and 13 mg, respectively, per kg body weight). Sternomastoid muscle exposure and NMJ imaging were performed as previously described (Akaaboune et al., 1999; Lichtman et al., 1987; van Mier and Lichtman, 1994). Briefly, the anesthetized mouse was placed on its back on the stage of a customized epifluorescence microscope, and NMJs were viewed under a coverslip with water immersion objectives (20 \times and 60 \times UAPO 0.7 NA, Olympus BW51, Optical Analysis Corporation, NH) and a digital CCD camera (Retiga EXi, Burnaby, BC, Canada). Mice were intubated and ventilated for the duration of the imaging sessions. For imaging at multiple time points, the mouse was sutured after each session and allowed to fully recover before the next imaging session.

Department of Molecular, Cellular and Developmental Biology and Neuroscience Program, University of Michigan, 830 North University Avenue, Ann Arbor, MI 48109, USA.

*Author for correspondence (e-mail: makaabou@umich.edu)

Labeling of distinct AChR pools

The labeling protocol was performed as previously described (Bruneau et al., 2005). Briefly, the sternomastoid muscle was bathed first with fully substituted bungarotoxin (BTX)-biotin (5 $\mu\text{g/ml}$, 1 hour; Molecular Probes, Eugene, OR) to label AChRs, and then with streptavidin conjugated to Alexa 488 (strept-488; green; 10 $\mu\text{g/ml}$, 3 hours; Molecular Probes) to saturate all biotin sites. To ensure that all biotin sites were saturated, a second, differently-colored label, streptavidin-Alexa 594 (strept-594; red; 10 $\mu\text{g/ml}$, 10-20 minutes) was added to the sternomastoid muscle, and the synapses imaged. The absence of strept-594 staining indicated that all biotin sites were initially saturated with strept-488. Three to 4 days later, the mouse was re-anesthetized, and the sternomastoid muscle re-exposed and bathed with strept-594 to label the AChRs that had recycled back to the muscle surface as AChR-BTX-biotin complexes. The muscle was washed out continuously for 15 minutes with Ringer's solution. A brief chase of unlabeled streptavidin (10 minutes) was added to the sternomastoid muscle to prevent the (unlikely) binding to recycled AChRs of any residual fluorescent streptavidin that remained in the milieu after the extensive washing. This labeling procedure would prevent any erroneous estimation of receptor removal. The doubly labeled superficial synapses were then imaged (IPLAB software, Scanalytics, VA). At subsequent time points, the same synapses were relocated and imaged. In this way, we were able to distinguish the pre-existing BTX-biotin-labeled receptors (retaining their initial streptavidin) from the recycled receptor pools. It is worth noting that at the time of recycled AChR labeling, a significant number of receptors in the NMJ are new, functional receptors, and these are sufficient to allow normal synaptic transmission (Bruneau et al., 2005; Lingle and Steinbach, 1988). All controls for the specificity of biotin-streptavidin dissociation were established previously by Bruneau et al. (Bruneau et al., 2005).

To determine the loss rate of newly synthesized receptors, the sternomastoid muscle was incubated with unlabeled BTX (5 $\mu\text{g/ml}$, 1.5 hours) to saturate all surface receptors (a second dose of fluorescent BTX was used to verify that all AChRs were saturated). Four to 5 days after initial labeling, newly inserted receptors were labeled with BTX-biotin at a sub-saturating dose (5 $\mu\text{g/ml}$ for 20 minutes), so that synaptic transmission remained functional, followed by a saturating dose of strept-488 (green). Superficial synapses were imaged and fluorescence loss was monitored over several days.

Surgical procedures

Sternomastoid muscles were denervated by excising a 5 mm piece of the sternomastoid nerve to prevent re-innervation. To determine the effect of denervation on the number of receptors recycled at the postsynaptic membrane, mice denervated 6-8 days earlier were anesthetized and the sternomastoid muscle was exposed and labelled first with BTX-biotin, and then with a single saturating dose of strept-594, and superficial synapses were imaged as described above. Three days later, the animal was re-anaesthetized, the same synapses were imaged and the loss of fluorescence measured. The sternomastoid muscle was bathed again with fresh strept-594 (to label recycled AChRs), synapses were imaged and the fluorescence intensity assayed. For comparison, a similar labeling protocol was applied to innervated synapses.

To determine the removal rate of recycled and pre-existing AChRs in denervated muscle, the sternomastoid muscle of mice denervated 6-8 days earlier was labeled with BTX-biotin, followed by a single saturating dose of strept-488. Three days later, the sternomastoid muscle was exposed and synapses labeled with a single saturating dose of strept-594 (to label all receptors that had recycled over that time); then, superficial synapses were imaged, their fluorescence intensities were measured, and the decrease in fluorescence of both AChR pools was monitored over time.

To determine the effect of muscle action potentials on AChR turnover, immediately after recycled receptor labeling in denervated NMJs, the muscle was directly stimulated with a Grass SD5 stimulator connected to two platinum wires placed either side of the muscle. The stimulus pulses (3 msecond bipolar pulses of 6-9 V at 10 Hz for 1 second duration every 2 seconds) elicited maximal twitching and therefore action potentials in all muscle fibers. Mice were continuously ventilated and maintained under

anesthesia by intraperitoneal injections of KX every 2 hours for the duration of the experiment. To minimize dehydration, a coverslip was placed over the exposed muscle.

Quantitative fluorescence imaging

The fluorescence intensity of labeled receptors at NMJs was assayed using a quantitative fluorescence imaging technique, as described by Turney and colleagues (Turney et al., 1996), with minor modifications. This technique incorporates compensation for image variation that may be caused by spatial and temporal changes in the light source and camera between imaging sessions, by calibrating the images with a non-fading reference standard. A key feature of the quantitative imaging approach used in the current study is that it involves repetitive imaging of the same fluorescent ligands (strept-594 and strept-488). Thus, as long as we verified that labeling had reached saturation and that the image pixel intensity was not saturated, it was relatively trivial to get an accurate quantitative measurement of the relative number of AChRs.

Pharmacology

For all agents tested, 500 μl of a stock solution was placed directly onto the sternomastoid muscle for 9 hours. During the experiment, the animal was intubated with a ventilator to avoid asphyxiation. To inhibit tyrosine phosphatase activity, we used two agents: phenylarsine oxide (2 mM; Sigma, St Louis, MO) and pervanadate (5-10 mM). Pervanadate solution was prepared by mixing 1.7% H_2O_2 and sodium orthovanadate (Sigma) in a ratio of 1:50 for 10 minutes before adding it to the sternomastoid muscle (Madhavan et al., 2005). Okadaic acid (10-100 μM ; Sigma) was used to inhibit serine/threonine phosphatases. To verify the effectiveness of okadaic acid *in vivo*, at the end of the imaging session the sternomastoid muscle that had been bathed with okadaic acid was removed from the mouse and homogenized in RIPA buffer (Sigma). The supernatant was then subjected to a direct fluorescence-based assay for detecting serine/threonine phosphatase activity (RediPlate™ 96 EnzChek serine/threonine phosphatases Assay Kit; Molecular Probes), according to the manufacturer's instructions. Briefly, appropriate buffers for the serine/threonine phosphatases PPI and PP2A were added to a 96-well microplate preloaded with inhibitors of phosphatases other than serine/threonine phosphatases, and with the fluorogenic serine/threonine phosphate substrate DiFMUP (6,8-difluoro-4-methyl-umbelliferyl phosphate), from which DiFMU is generated. DiFMUP was then fully solubilized and homogenates from treated and untreated muscle were added to the wells. The fluorescence emitted by DiFMU was measured using a fluorescence microplate reader, with excitation at 355 ± 20 nm and emission at 460 ± 12.5 nm.

Confocal microscopy

The sternomastoid muscle was saturated with BTX-biotin followed by a single saturating dose of strept-488 (10 $\mu\text{g/ml}$, 3 hours). Three to 4 days later, the animal was re-anaesthetized and strept-594 was added to the sternomastoid muscle to label recycled AChRs. Two to 3 days later, the animal was perfused transcardially with 2% paraformaldehyde (PFA) and the sternomastoid muscle removed and longitudinally sectioned. Muscle sections (20 μm) were blocked with 10% BSA and 0.5% Triton X-100, and then bathed with monoclonal anti-receptor antibody (mAb 35; Developmental Studies Hybridoma Bank, Iowa University, IA), followed by an anti-rat secondary antibody conjugated to Alexa 647 (Molecular Probes). Muscle sections were scanned with a confocal microscope (Olympus fluoview) and imaged. The z-stacks were then collapsed and the contrast adjusted with Photoshop to maximally resolve intracellular fluorescent spots.

RESULTS

Recycled and pre-existing AChR removal at the NMJ of live mice

Recent work from our laboratory has shown that a significant number of receptors recycle back to synapses after internalization (Bruneau et al., 2005), and we wanted to know whether recycled receptors are as stable in the synapse as pre-existing receptors (receptors retaining their strept-488 after initial labeling). To test this, the sternomastoid muscle of live mice was labeled with BTX-

biotin, followed by a single saturating dose of strept-488 to saturate all biotin sites. To ensure that all biotin sites were labeled, the muscle was exposed to the differently-colored strept-594. Images of superficial synapses showed no staining with strept-594, indicating that all biotin sites were saturated with strept-488. The animal was then allowed to recover. Three to 4 days after the initial labeling, strept-594 was added to label recycled receptors that had lost their strept-488 label but retained BTX-biotin, and images were taken immediately (day 0). The dissociation of streptavidin from AChR-BTX-biotin does not occur spontaneously on the muscle surface, but rather only after the complex (AChR-BTX-biotin/strept-488) is internalized (Bruneau et al., 2005). Pre-existing AChRs that retain

BTX-biotin/strept-488 after the initial labeling and recycled AChRs labeled with BTX-biotin/strept-594 could then be imaged separately, and the changes in their fluorescence intensities monitored over time. As shown in Fig. 1A, recycled and pre-existing AChRs intermingled in the same postsynaptic membrane. One to 3 days after labeling recycled AChRs with strept-594, both recycled and pre-existing AChRs were re-imaged, once or multiple times, and then their fluorescence intensities assayed. We found that after 1 day, the fluorescence intensity of recycled receptors (receptors tagged with BTX-biotin/strept-594) decreased to 59% (± 5 s.d., $n=25$) of their original fluorescence, which corresponds to a half-life of ~ 1.3 days. At 2 and 3 days, the remaining fluorescence intensities were 36% (± 6 s.d., $n=20$) and 16% (± 2 s.d., $n=15$) of the original fluorescence, respectively. However, at the same synapses over the same times, the fluorescence intensity of AChRs labeled with BTX-biotin/strept-488 decreased to only 84% (± 6 s.d., $n=20$) of the original fluorescence after 1 day (half-life ~ 4 days), and after 2 and 3 days the fluorescence had decreased to 68% (± 9 s.d., $n=10$) and 54% (± 4 s.d., $n=15$), respectively (Fig. 1B,C). Similar results were obtained if strept-594 was used initially to label pre-existing receptors and strept-488 to label recycled AChRs.

To examine the removal rate of newly inserted receptors, the sternomastoid muscle was saturated with BTX and the animal allowed to recover. Four to 5 days later, the sternomastoid muscle was bathed with a low dose of BTX-biotin/strept-488 to label newly synthesized receptors. The superficial synapses were imaged and then re-imaged 1 and 2 days later. We found that the fluorescence from newly synthesized receptors decreased to 79% (± 5 s.d., $n=14$) of the original fluorescence after 1 day, and to 69% (± 10 s.d., $n=7$) after 2 days. These data indicate that the removal rate of newly synthesized receptors is significantly slower than for recycled receptors ($P < 0.0001$).

Given the rapid loss of recycled receptors from the postsynaptic membrane, we next examined whether this loss is matched by the insertion of new recycled receptors over the same time period. The sternomastoid muscle of three mice was labeled with BTX-biotin followed by a saturating dose of strept-488. Three to 4 days later the animal was anaesthetized and the sternomastoid muscle bathed with a saturating dose of strept-594 to label the recycled receptors, as described above. The superficial synapses were then imaged, and the animal was allowed to recover. Two days later, the same synapses were re-imaged and the fluorescence of each synapse measured at each data point. The sternomastoid muscle was then bathed with a saturating dose of fresh strept-594 to label receptors that had been recycled over the given time period. When we measured the fluorescence intensity at 2 days, we found the fluorescence remaining from the recycled pool (labeled with strept-594) was 35% (± 6 s.d., $n=17$) of the original fluorescence. When re-labeled with new strept-594, the fluorescence intensity returned to 99% (± 17 s.d., $n=10$) of the initial recycled AChR fluorescence (Fig. 2A,B). This indicates that the insertion of new recycled receptors matches the loss of recycled receptors from the postsynaptic membrane.

Targeting of recycled AChRs to stable fluorescent intracellular vesicles after internalization

We have previously shown that receptors that are removed from synapses are internalized in intracellular endocytic vesicles (Akaaboune et al., 1999; Bruneau et al., 2005). Because recycled and pre-existing receptors intermingle at the same postsynaptic membrane but turn over at such different rates (Fig. 1), we wanted to know whether recycled and pre-existing receptors, after their

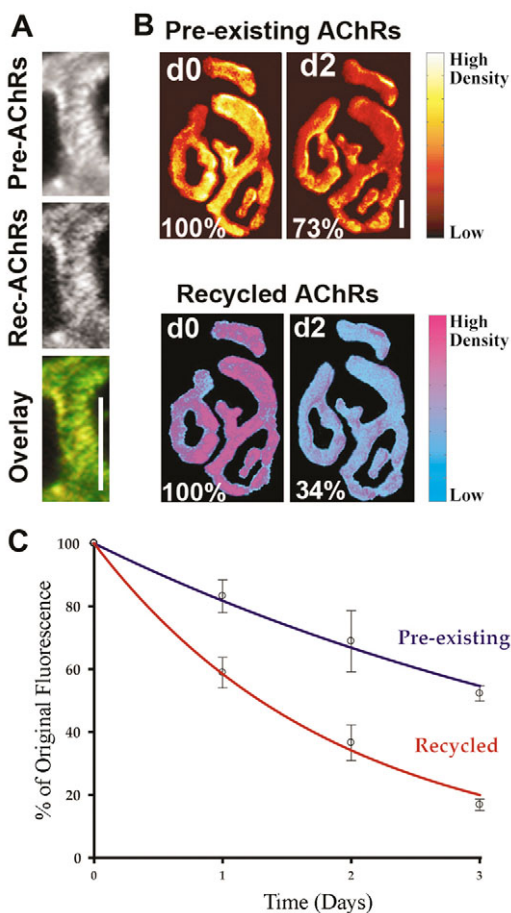


Fig. 1. Recycled and pre-existing AChRs are removed at different rates from the same synapse.

The sternomastoid muscle was labeled first with BTX-biotin/strept-488, then 3–4 days later with strept-594 to selectively label recycled AChRs. (A) High resolution image of a NMJ branch showing that recycled (red and yellow overlay) and pre-existing (retaining their strept-488 after initial labeling; green and yellow overlay) AChRs are intermingled in the postsynaptic membrane. (B) Pre-existing and recycled AChRs labeled with different fluorophores were assayed for fluorescence intensities immediately after strept-594 labeling of recycled AChRs (d0), and 2 days later (d2). The total fluorescence intensity of each AChR pool was normalized to 100% at initial imaging. Pseudo-color images provide a linear representation of the density of AChRs. (C) Graph summarizing the results obtained from all junctions by the approach shown in B. Each data point represents the mean percentage of fluorescence intensity \pm s.d. Note that recycled receptors are removed significantly faster than pre-existing receptors. Scale bars, 20 μ m.

removal from the postsynaptic membrane, are internalized in the same or in distinct intracellular vesicles. To examine this, the sternomastoid muscle was labeled with BTX-biotin/strept-488 (green), and 3–4 days later the recycled receptors were labeled with strept-594 (red). When recycled and pre-existing AChRs were re-imaged 2 or more days later, we were surprised to find that all the vesicles that contained red fluorescence from recycled receptors also contained green fluorescence from pre-existing receptors ($n=50$ synapses; Fig. 3A). This prompted us to monitor the formation and accumulation of both green and red intracellular puncta using time-lapse imaging. The sternomastoid muscle was labeled with BTX-biotin/strept-488, and 3–4 days later the receptors that had recycled over this time were labeled with strept-594. When superficial synapses were imaged immediately after strept-594 (red) labeling, the AChRs labeled with green strept-488 were concentrated in the postsynaptic membrane and in internal compartments visualized as small spots of fluorescence in the vicinity of the junction (Fig. 3B,

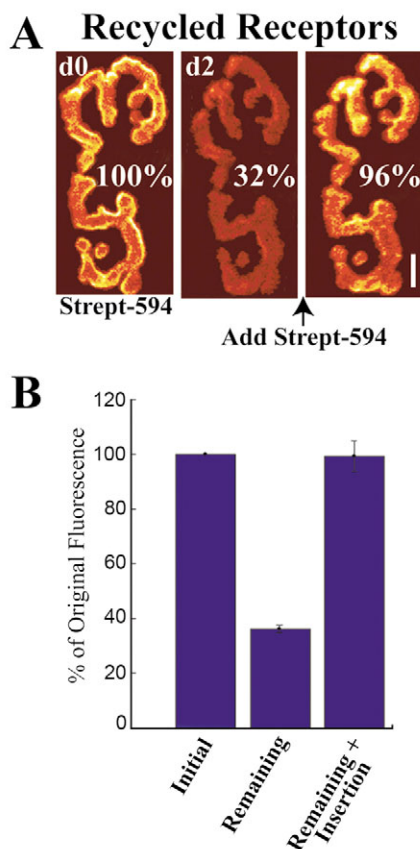


Fig. 2. Insertion of newly recycled AChRs matches the removal of recycled receptors. (A) The sternomastoid muscle was labeled with BTX-biotin followed by a saturating dose of strept-488. Three to 4 days later, the animal was anaesthetized and the sternomastoid muscle bathed with a saturating dose of strept-594 to specifically label the recycled receptors; superficial synapses were imaged immediately, and again 2 days later, and the loss of recycled receptors determined. The sternomastoid muscle was then bathed with fresh strept-594, and the synapses re-imaged to determine the insertion of newly recycled AChRs. Scale bar, 20 μm . (B) Bar graph summarizing the recycled AChR loss and insertion results (\pm s.d.) obtained by the approach shown in A. Note that nearly all of the AChRs from the recycled pool lost over the 2 days were replaced by newly recycled receptors re-inserted into the postsynaptic membrane of the NMJ.

top panels). When the same synapse was imaged 8 hours later, some of the green spots remained whereas others had disappeared. At this time point, faint red fluorescent spots began to appear, but only at the stable spots of green fluorescence (Fig. 3B, middle panels). After 28 hours, although many of the green fluorescent spots had disappeared, stable spots that contained both strept-488 and strept-594 remained (Fig. 3B, bottom panels). These results indicate either that the removed recycled receptors were directly and specifically targeted to stable vesicles already containing internalized AChR-BTX-biotin/strept-488 complexes, or that the fluorescent puncta observed in the intracellular vesicles were from streptavidin-Alexa tags that had been removed from both receptor pools after internalization (see Discussion).

If the red and green fluorescence observed in stable vesicles derives from streptavidin-Alexa tags that have been removed from their receptor complexes and then sequestered, then we would expect at least a subset of these vesicles to lack AChRs. To investigate this possibility, the sternomastoid muscle was labeled with BTX-biotin/strept488 (green), and three days later incubated with strept-594 (red) to label recycled receptors. Two days later, the animal was perfused with PFA and the muscle dissected, sectioned and immunostained with the anti-AChR antibody mAb 35 (pseudo-colored blue). Interestingly, some green and red fluorescent vesicles were devoid of receptors (Fig. 4), suggesting that the streptavidin-Alexa tags had indeed been removed and

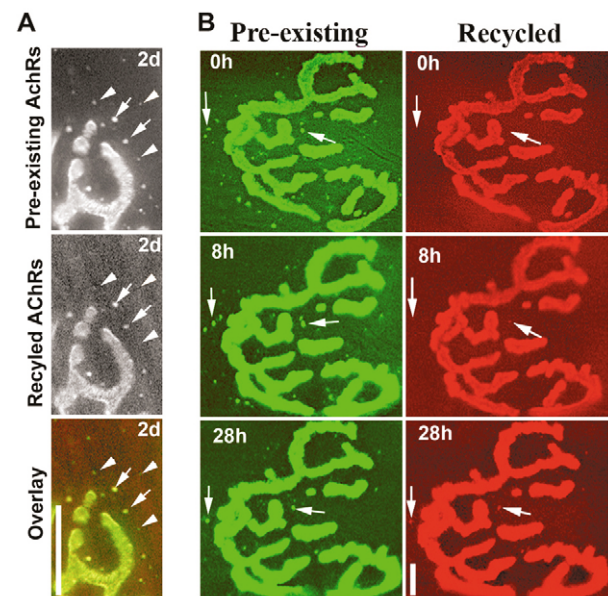
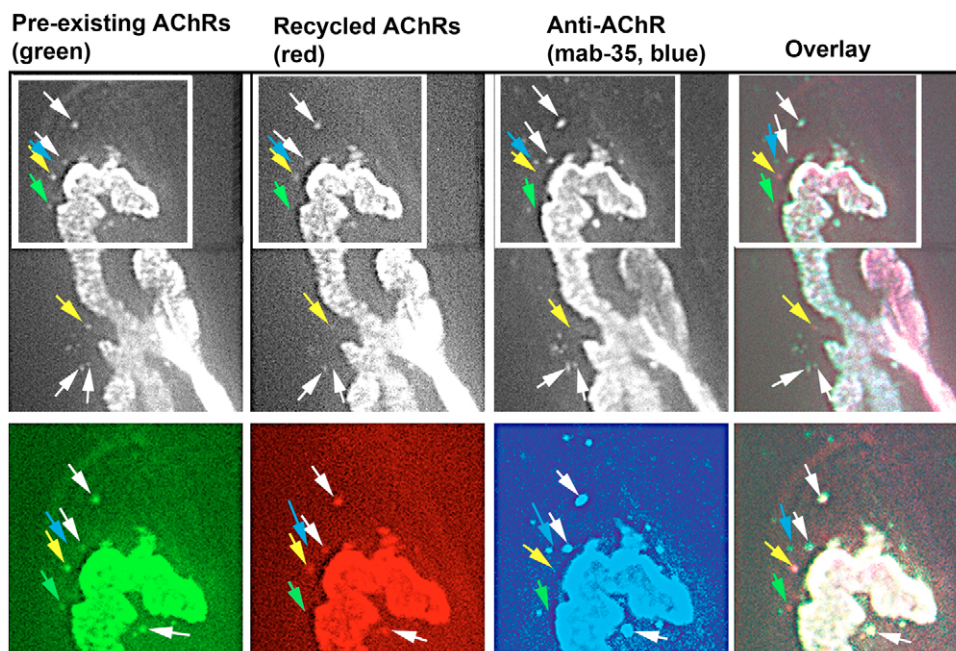


Fig. 3. Fluorescent tags from recycled receptors are endocytosed and targeted to vesicles containing strept-488 from pre-existing AChRs. The sternomastoid muscle was labeled first with BTX-biotin/strept-488, then 3 days later with strept-594 to label recycled receptors. (A) Recycled and pre-existing AChRs imaged 2 days after recycled receptor labeling. Note that all the vesicles containing red fluorescence from recycled AChRs also have green signals from pre-existing AChRs (arrows), whereas some of the green spots lack red signal (arrowheads). (B) A NMJ was labeled as in A and then imaged periodically over the next 28 hours. Note that a number of the vesicles containing strept-488 from the pre-existing AChRs at time 0 are stable over the next 28 hours (arrows), whereas others are transient. The strept-594 labels from recycled receptors are selectively targeted to the stable vesicles containing fluorescent label from pre-existing receptors. Scale bars, 20 μm .

Fig. 4. Confocal images of a triply labeled NMJ.

The sternomastoid muscle of a live animal was first labeled with BTX-biotin/strept-488 (green), then 3 days later with strept-594 (red) to label recycled receptors. Two days after recycled receptor labeling, the animal was perfused with 2% PFA, the sternomastoid muscle sectioned and immunostained with anti-AChR. Green arrows indicate accumulation of green fluorescent streptavidin that has been removed from pre-existing AChRs after internalization, which may correspond to degradative vesicles. Yellow arrows indicate accumulation of green and red streptavidin tags removed from pre-existing and recycled receptors after internalization, which probably also correspond to degradative vesicles. Blue arrows indicate vesicles containing AChRs, but lacking any streptavidin-Alexa tags; these vesicles may correspond to internalized AChRs

in later stages of recycling and/or degradation, or newly synthesized receptors in the process of insertion. White arrows indicate vesicles containing receptors and their streptavidin tags after internalization. Colors in the overlay have been adjusted in Photoshop (Adobe) to maximize contrast. Boxed areas (above) are enlarged below. The results suggest that the vesicles containing fluorescent products (yellow arrows) may be stable, whereas those corresponding to cycling AChRs (white arrows) may be more dynamic. Scale bar, 20 μm .



sequestered, possibly in degradative vesicles. Other vesicles contained fluorescent streptavidin-Alexa tags and receptors, possibly indicating complexes that were in the process of recycling or degradation. A third subset of puncta contained receptors only, without any fluorescent streptavidin tags, indicating receptors in the process of insertion, or receptors in the later stages of recycling that already had their streptavidin-Alexa tags removed (Fig. 4).

Effect of denervation and muscle stimulation on recycled AChR dynamics

Given the rapid removal rate of recycled AChRs, we next investigated whether this loss rate could be further affected by muscle denervation. We first tested whether denervation has any effect on the insertion of recycled AChRs into the postsynaptic membrane. Innervated NMJs and junctions denervated 6-8 days earlier were labeled with a single saturating dose of BTX-biotin, and then all biotin sites were saturated with strept-594 (red). The superficial synapses were imaged and 3 days later the same synapses were located and re-imaged to measure the loss of fluorescence. To quantify the number of recycled AChRs that had been inserted after initial labeling, new strept-594 (red) was added to the sternomastoid muscle and the same synapses were re-imaged. Interestingly, we found that only 8% (± 3.8 s.d., $n=20$) of the original fluorescence had recovered at denervated synapses after 3 days (Fig. 5A,B), which is significantly less than the insertion rate of recycled receptors in innervated junctions (25% of original fluorescence ± 7.1 s.d., $n=20$; Fig. 5C,D).

Next, we investigated whether recycled and pre-existing AChRs have similar removal rates in denervated muscle. Junctions denervated 6-8 days earlier were labeled with BTX-biotin/strept-488 and the animals allowed to recover. Three days later, the recycled AChRs were labeled with strept-594, and superficial synapses were

imaged immediately and then re-imaged 1 and 2 days later. We found that after only 1 day, the strept-594 fluorescence intensity (labeled recycled AChRs) decreased dramatically to just 35% (± 5 s.d., $n=17$) of the original fluorescence (corresponding to a half-life of ~ 15 hours, nearly twice as fast as the half-life of recycled AChRs at innervated synapses). Loss of fluorescence continued, decreasing to 16% (± 3 s.d., $n=9$) after 2 days. At the same time, the strept-488 fluorescence from pre-existing receptors decreased to 70% (± 6 s.d., $n=10$) after 1 day (half-life ~ 1.9 days, also nearly two times faster than the half-life at innervated synapses), and to 43% (± 6 s.d., $n=9$) of their original fluorescence after 2 days (Fig. 6A,B). These results indicate that denervation increases the already rapid removal of recycled receptors from the postsynaptic membrane, and has a similar effect on both recycled and pre-existing AChRs, nearly doubling the rate of removal of each receptor pool.

Because the above experiments indicate that muscle activity is important for receptor stability, we next tested whether direct muscle stimulation could prevent the rapid removal of recycled AChRs from the postsynaptic membrane. Denervated sternomastoid muscle was saturated (6-8 days after denervation) with BTX-biotin/strept-488, and then 3 days later was saturated with strept-594 to specifically label recycled AChRs. Superficial synapses were imaged and muscle action potentials were then elicited via stimulating electrodes placed at either end of the muscle (3 msecond bipolar pulses of 6-9 V at 10 Hz for 1 second every 2 seconds for the entire 8 hour period). For the duration of the experiment, the mouse was intubated and ventilated to prevent asphyxia. The result was dramatic: the loss of recycled AChRs observed in denervated muscles over the 8 hours (66% of original fluorescence remaining ± 5 s.d., $n=8$) was almost completely prevented by the stimulation of denervated muscles (94% of original fluorescence remaining ± 6 s.d., $n=16$) (Fig. 7A-C). This indicates that muscle action potentials are sufficient to prevent the loss of recycled receptors.

Proper localization of recycled receptors requires tyrosine phosphatase activity

Because phosphorylation and dephosphorylation events are associated with postsynaptic receptor cycling in central synapses (Ehlers, 2000; Esteban et al., 2003; Malinow and Malenka, 2002), we next tested whether AChR recycling also depends upon phosphorylation/dephosphorylation events. The sternomastoid muscle was labeled with BTX-biotin/strept-488 (green), and the muscle then bathed continuously in a phosphatase inhibitor. The mice were anesthetized and ventilated to prevent asphyxia. After a 9-hour incubation with the drug, strept-594 (red) was added to the sternomastoid muscle to label receptors that had been recycled back to the membrane after initial labeling. We found a striking alteration in receptor localization at synapses when the muscle was treated with phenylarsine oxide (PAO), a known inhibitor of tyrosine phosphatases (Fletcher et al., 1993; Moulton et al., 2006; Moulton et al., 2002). In contrast to untreated control muscles, where the recycled surface receptors were restricted to the junctional area as were the

original receptors, PAO treatment resulted in red labeling in the peri-synaptic region as well as the junctional region (Fig. 8B,C). The presence of red signal in the peri-synaptic region is specific to recycled receptors labeled with strept-594 (red), because at 9 hours no pre-existing receptors (green) were detected outside of the original synapse (Fig. 8A). Treatment with another common tyrosine phosphatase inhibitor, pervanadate (Madhavan et al., 2005; Moulton et al., 2006), caused the same peri-synaptic staining of recycled AChRs (Fig. 8E,F), without affecting the synaptic localization of pre-existing AChRs (Fig. 8D). These results indicate that tyrosine phosphatase activity is involved in the correct localization of recycled receptors.

To investigate the potential role of serine/threonine phosphatases in receptor recycling, the sternomastoid muscle of four mice was labeled (as described above) and then bathed in different concentrations of okadaic acid (10–100 μ M), a specific inhibitor of serine/threonine phosphatases PP1 and PP2A (Pahan et al., 1998). Nine hours later, when the muscle was labeled with strept-594,

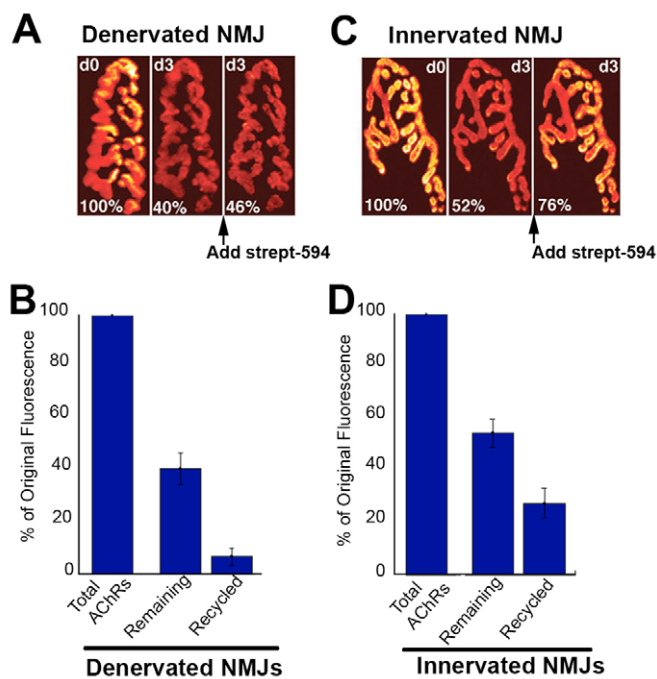


Fig. 5. Muscle denervation affects the contribution of recycled AChRs. (A) A denervated NMJ was labeled with BTX-biotin/strept-594 and imaged immediately. Three days later the synapse was re-imaged to measure the loss of fluorescence, then incubated with strept-594 to selectively label recycled AChRs. Note that 60% of the original fluorescence was lost after 3 days, whereas very little fluorescence was gained after strept-594 was added (6% of the original fluorescence), indicating that recycling of AChR is significantly decreased in denervated muscle. All three panels are displayed on the same intensity scale. (B) Bar graph summarizing the mean percentage of fluorescence intensity \pm s.d. obtained from many denervated junctions. (C) An innervated synapse treated as in A, showing that a significant number of recycled AChRs return back to the postsynaptic membrane. (D) Bar graph summarizing measurements obtained from many innervated synapses.

A Denervated Recycled Receptors

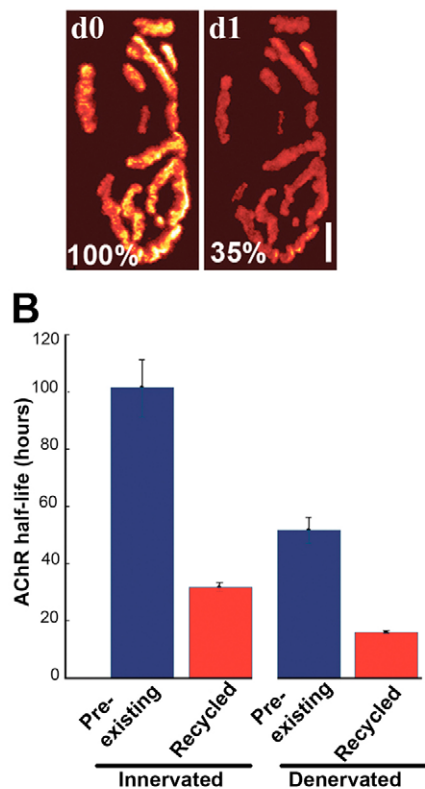


Fig. 6. Denervation increases the removal rates of recycled and pre-existing AChRs at the NMJ. (A) AChRs at denervated NMJs were first labeled with BTX-biotin/strept-488, and 3 days later recycled AChRs were labeled with strept-594. Fluorescence signals from both receptor pools were then imaged, and re-imaged 1 day later. (B) Bar graph showing the lifetime of recycled and pre-existing AChRs from the same synapses as assessed by the change in fluorescence over the 1-day period. In innervated synapses, recycled AChRs had an average half-life of 28 hours, whereas pre-existing AChRs had an average half-life of ~102 hours. In denervated synapses, recycled AChR half-life dropped to ~15 hours, and pre-existing AChR half-life decreased by the same proportion to ~48 hours. Scale bar: 20 μ m.

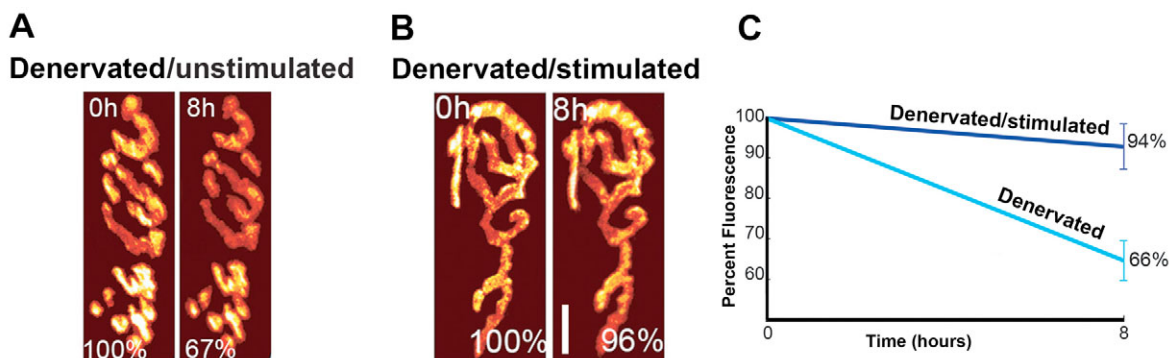


Fig. 7. Muscle stimulation prevents loss of recycled AChRs from denervated NMJs. Three days after labeling with BTX-biotin/strept-488, recycled AChRs on denervated muscle were labeled with strept-594 and imaged immediately, and then again after 8 hours in the absence (**A**) and presence (**B**) of stimulation. Scale bar, 20 μm . (**C**) Graph summarizing the fluorescence measurements obtained from many synapses. After 8 hours, ~66% of fluorescence from recycled receptors remained in denervated synapses; however, when denervated muscle was chronically stimulated, this loss of fluorescence was largely abolished.

specific staining was observed only in the junctional zone, indicating that the targeting of recycled receptors does not require serine/threonine phosphatases (Fig. 8G-I). The effectiveness of this drug in vivo was tested at the end of the imaging session by removing and homogenizing the sternomastoid muscle, and testing the activity of PP1 and PP2A phosphatases using a serine/threonine phosphatase assay kit. When the muscle was incubated in 10 μM okadaic acid, most of the serine/threonine phosphatase activity (>70%) was inhibited, when compared with untreated muscle. When 100 μM okadaic acid was used, all serine/threonine phosphatase activity was inhibited and the muscle also showed signs of swelling.

DISCUSSION

In this study, we report that at fully functional synapses recycled AChRs turn over more rapidly than pre-existing or newly synthesized AChRs that are colocalized in the same postsynaptic membrane. The absence of muscle activity significantly decreases the number of recycled AChRs and increases the already rapid removal rate of recycled AChRs, whereas direct muscle stimulation completely prevents receptor loss. In addition, this work provides evidence for a possible involvement of tyrosine dephosphorylation in the insertion or maintenance of recycled AChRs at synaptic sites.

An interesting finding of this work is that the lifetime of recycled receptors is far shorter than that of the pre-existing AChRs, even though all of these AChRs are intermingled in the same postsynaptic membrane. It is unlikely that the difference in receptor lifetime obtained in our studies is due to BTX binding itself, as we are comparing the removal rates of receptors that are both tagged with BTX. However, it must be acknowledged that the use of BTX, which specifically and irreversibly binds to AChRs, also blocks AChR function. Although there is no direct evidence as to whether BTX binding itself changes the behavior of AChRs, a number of previous studies suggest that labeled receptors behave normally as long as NMJ activity is not totally blocked (Akaaboune et al., 1999; Lingle et al., 1988). Although it has been shown previously that the gamma and epsilon subunits of AChRs are able to turn over at different rates, it is unlikely that the differences in loss rates are due to differences in the subunit composition of receptors (gamma versus epsilon) because innervated adult synapses only express the epsilon subunit (Burden, 1977; Missias et al., 1996; Yumoto et al., 2005). This implies that an unknown mechanism exists that specifically alters recycled AChR stability.

It is possible that during the process of intracellular receptor trafficking (in early endosomes or specialized recycling endosomes), alteration or modification of AChR subunits or receptor-associated proteins may occur. Such alterations might affect the interaction of receptors with postsynaptic scaffolding proteins, which in turn may affect their stability once inserted into the postsynaptic membrane. For example, it has been suggested that phosphorylation events are involved in the stabilization of AChRs (Caroni et al., 1993), and inhibition of these events has been shown to increase receptor removal and prevent receptor clustering, despite ongoing muscle activity (Ferns et al., 1996; Fuhrer et al., 1997; Wallace, 1994; Wallace et al., 1991). At central synapses, it has been shown that a coordination of phosphorylation and dephosphorylation events may regulate synaptic strength (Moult et al., 2006; Raymond et al., 1993; Raymond et al., 1994; Roche et al., 1994); it is possible that similar mechanisms may be involved at the NMJ. This possibility is supported by our results, which show that inhibition of tyrosine phosphatase activity can cause selective disruption of receptor recycling, resulting in labeling outside of the usually sharp NMJ boundary, whereas pre-existing receptors remain intact within the NMJ. This suggests that the phosphorylation of receptors or associated proteins at tyrosine sites during trafficking might cause a mistargeting of recycled receptors or increase their mobility once they have recycled into the postsynaptic membrane. It is also conceivable that tyrosine phosphatase inhibitors could selectively increase the insertion and accumulation of recycled receptors at the peri-junctional region. Interestingly, the same observation has been made previously in the synapses of frog nerve/muscle co-cultures treated with tyrosine phosphatase inhibitors, where it was attributed to the dissociation and migration of pre-existing receptors into the peri-synaptic region (Dai and Peng, 1998). Because we were able to distinguish between pre-existing and recycled pools of receptors, our results suggest that tyrosine phosphatase inhibition does not cause dissociation of pre-existing receptors, but rather that it specifically interferes with the delivery of internalized receptors back into the NMJ or with their maintenance at the postsynaptic membrane.

Muscle activity appears to be crucial for the insertion and stability of recycled AChRs in the postsynaptic membrane. Our results indicate that the contribution of recycled AChRs is significantly depressed in denervated muscle synapses when compared with innervated synapses. However, the inhibition of recycling is not affected within the first week of denervation (data not shown). It is possible that during the first week of muscle denervation, the

insertion of recycled receptors is maintained by spontaneous release of acetylcholine neurotransmitter by Schwann cells (Brett et al., 1982; Dennis and Miledi, 1974), which might explain why the number of synaptic receptors only begins to decline ~9 days after muscle denervation (Andreose et al., 1995). Consistent with this proposal, we have previously shown that spontaneous release of a neurotransmitter is sufficient to prevent the loss of receptors from synapses (Akaaboune et al., 1999). This suggests that the decrease in receptor number at denervated muscle synapses over time could be attributed to a decrease in the delivery of the recycled receptor pool back to the postsynaptic membrane. Interestingly, the absence

of muscle activity following denervation not only increases the removal rate of pre-existing AChRs, but also accelerates the already rapid removal of the receptors that have recycled back into the membrane. This indicates that recycled receptors, despite their rapid loss, can still be controlled by synaptic activity. In agreement with our previous findings, which showed that the stimulation of denervated muscle prevents the removal of pre-existing AChRs (Bruneau et al., 2005), in the present study we found that muscle stimulation also prevents the removal of recycled receptors. Consistent with these results, muscle stimulation alone has been reported to reversibly increase the metabolic stability of receptors at synapses that are denervated early in development, and can prevent the decrease in AChR half-life observed at surgically denervated and blocked endplates (Akaaboune et al., 1999; Brenner and Rudin, 1989; Rotzler and Brenner, 1990). However, the way in which neuromuscular transmission or muscle action potentials regulate AChR behavior is not understood. It is possible that muscle contraction caused by direct stimulation causes an increase in calcium influx through either ligand-gated or L-type channels, or that it causes calcium release directly from intracellular stores. In support of this idea, previous studies have shown that blockade of L-type channels affects AChR stability (Rotzler et al., 1991).

At functional neuromuscular synapses, recycled receptors are continually inserted into the postsynaptic membrane. However, it is unclear what proportion of the recycled receptor pool derives from pre-existing or previously recycled AChRs, or how many times receptors are able to recycle back to the membrane before being degraded. If receptors recycle only once, then a fraction of the pre-existing pool must enter the recycling pathway over time to maintain the recycled receptor pool. An intriguing observation is that red streptavidin from recycled AChRs colocalizes in intracellular vesicles with the previously internalized green fluorescent label from pre-existing receptors (see Figs 3, 4). This raises two possibilities. First, recycled AChRs could have a tag that directly shuttles them to stable degradation vesicles containing previously internalized pre-existing AChRs. In this scheme, it is tempting to speculate that the stable spots of fluorescence are part of the accumulated degradation products, implying that AChRs might recycle only once before being targeted for degradation. Second, AChRs might recycle more than once and so the stable fluorescent vesicles may correspond to an accumulation of fluorescent tag that the recycled and pre-existing AChRs lose intracellularly while in the process of recycling. The absence of receptors in some vesicles suggests that these are indeed sites of degradation, which may correspond to stable vesicles observed in time-lapse imaging; the more dynamic vesicles are either in the process of recycling or are at an early stage in the degradation pathway. Although this result suggests that receptors may be recycled many times, losing their streptavidin tag each time, the question of how many times a receptor can be recycled before being degraded remains unresolved and requires the development of new study techniques.

This work was supported by the University of Michigan, National Institute of Neurological Disorders and Stroke Research Grant NS047332 (M.A.). We thank Isabel Martinez and David Sutter for their technical help and Drs John Kuwada, Richard Hume and Hans Brenner for helpful discussions. We also thank the Developmental Studies Hybridoma Bank for providing antibodies.

REFERENCES

- Akaaboune, M., Culican, S. M., Turney, S. G. and Lichtman, J. W. (1999). Rapid and reversible effects of activity on acetylcholine receptor density at the neuromuscular junction in vivo. *Science* **286**, 503-507.
- Andreose, J. S., Fumagalli, G. and Lomo, T. (1995). Number of junctional acetylcholine receptors: control by neural and muscular influences in the rat. *J. Physiol.* **483**, 397-406.

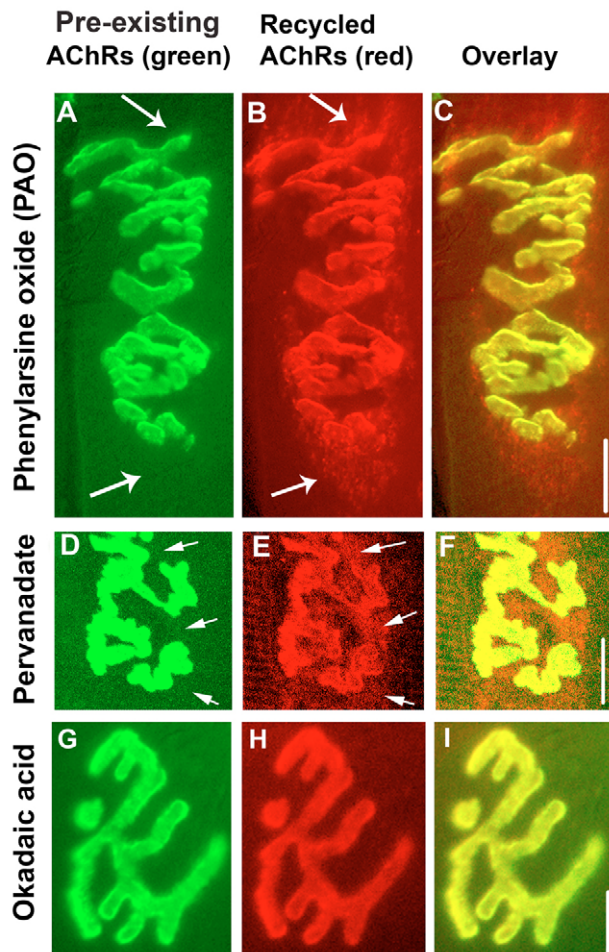


Fig. 8. Tyrosine phosphatase inhibition causes the accumulation of recycled receptors in the peri-synaptic membrane. (A) Live adult mouse NMJ previously saturated with BTX-biotin/strept-488 (green) at time 0 and viewed at high detector gain 9 hours later. The muscle was continuously bathed in the tyrosine phosphatase inhibitor PAO for 9 hours and then imaged. (B) The junction was then incubated with strept-594 (red) to determine if PAO affects AChR recycling. Peri-synaptic areas were labeled (arrows), indicating that some of the recycled receptors had become mistargeted. (C) Overlay of pre-existing and recycled receptors (overlay images were adjusted for brightness and contrast using Photoshop). (D-F) Similar results were obtained using an alternative tyrosine phosphatase inhibitor, pervanadate. Note that whereas recycled receptors (red) appear in the peri-synaptic area, pre-existing receptors (green) remain restricted to the synapse. (G-I) When the serine/threonine phosphatase inhibitor okadaic acid was used instead, recycled receptors (red) were properly targeted to the synapse. Scale bars: 20 μ m.

- Brenner, H. R. and Rudin, W.** (1989). On the effect of muscle activity on the end-plate membrane in denervated mouse muscle. *J. Physiol.* **410**, 501-512.
- Brett, R. S., Younkin, S. G., Konieczkowski, M. and Slugg, R. M.** (1982). Accelerated degradation of junctional acetylcholine receptor-alpha-bungarotoxin complexes in denervated rat diaphragm. *Brain Res.* **233**, 133-142.
- Bruneau, E., Sutter, D., Hume, R. I. and Akaaboune, M.** (2005). Identification of nicotinic acetylcholine receptor recycling and its role in maintaining receptor density at the neuromuscular junction in vivo. *J. Neurosci.* **25**, 9949-9959.
- Burden, S.** (1977). Acetylcholine receptors at the neuromuscular junction: developmental change in receptor turnover. *Dev. Biol.* **61**, 79-85.
- Caroni, P., Rotzler, S., Britt, J. C. and Brenner, H. R.** (1993). Calcium influx and protein phosphorylation mediate the metabolic stabilization of synaptic acetylcholine receptors in muscle. *J. Neurosci.* **13**, 1315-1325.
- Carroll, R. C., Lissin, D. V., von Zastrow, M., Nicoll, R. A. and Malenka, R. C.** (1999). Rapid redistribution of glutamate receptors contributes to long-term depression in hippocampal cultures. *Nat. Neurosci.* **2**, 454-460.
- Contractor, A. and Heinemann, S. F.** (2002). Glutamate receptor trafficking in synaptic plasticity. *Sci. STKE* **2002**, RE14.
- Dai, Z. and Peng, H. B.** (1998). A role of tyrosine phosphatase in acetylcholine receptor cluster dispersal and formation. *J. Cell Biol.* **141**, 1613-1624.
- Dennis, M. J. and Miledi, R.** (1974). Electrically induced release of acetylcholine from denervated Schwann cells. *J. Physiol.* **237**, 431-452.
- Ehlers, M. D.** (2000). Reinsertion or degradation of AMPA receptors determined by activity-dependent endocytic sorting. *Neuron* **28**, 511-525.
- Esteban, J. A., Shi, S. H., Wilson, C., Nuriya, M., Huganir, R. L. and Malinow, R.** (2003). PKA phosphorylation of AMPA receptor subunits controls synaptic trafficking underlying plasticity. *Nat. Neurosci.* **6**, 136-143.
- Ferns, M., Deiner, M. and Hall, Z.** (1996). Agrin-induced acetylcholine receptor clustering in mammalian muscle requires tyrosine phosphorylation. *J. Cell Biol.* **132**, 937-944.
- Fletcher, M. C., Samelson, L. E. and June, C. H.** (1993). Complex effects of phenylarsine oxide in T cells. Induction of tyrosine phosphorylation and calcium mobilization independent of CD45 expression. *J. Biol. Chem.* **268**, 23697-23703.
- Fuhrer, C., Sugiyama, J. E., Taylor, R. G. and Hall, Z. W.** (1997). Association of muscle-specific kinase MuSK with the acetylcholine receptor in mammalian muscle. *EMBO J.* **16**, 4951-4960.
- Gardner, J. M. and Fambrough, D. M.** (1979). Acetylcholine receptor degradation measured by density labeling: effects of cholinergic ligands and evidence against recycling. *Cell* **16**, 661-674.
- Grady, R. M., Akaaboune, M., Cohen, A. L., Maimone, M. M., Lichtman, J. W. and Sanes, J. R.** (2003). Tyrosine-phosphorylated and nonphosphorylated isoforms of alphasystrobrevin: roles in skeletal muscle and its neuromuscular and myotendinous junctions. *J. Cell Biol.* **160**, 741-752.
- Hayashi, Y., Shi, S. H., Esteban, J. A., Piccini, A., Poncer, J. C. and Malinow, R.** (2000). Driving AMPA receptors into synapses by LTP and CaMKII: requirement for GluR1 and PDZ domain interaction. *Science* **287**, 2262-2267.
- Huganir, R. L., Miles, K. and Greengard, P.** (1984). Phosphorylation of the nicotinic acetylcholine receptor by an endogenous tyrosine-specific protein kinase. *Proc. Natl. Acad. Sci. USA* **81**, 6968-6972.
- Lee, H. K., Barbarosie, M., Kameyama, K., Bear, M. F. and Huganir, R. L.** (2000). Regulation of distinct AMPA receptor phosphorylation sites during bidirectional synaptic plasticity. *Nature* **405**, 955-959.
- Lee, S. H., Simonetta, A. and Sheng, M.** (2004). Subunit rules governing the sorting of internalized AMPA receptors in hippocampal neurons. *Neuron* **43**, 221-236.
- Li, M. X., Jia, M., Yang, L. X., Jiang, H., Lanuza, M. A., Gonzalez, C. M. and Nelson, P. G.** (2004). The role of the theta isoform of protein kinase C (PKC) in activity-dependent synapse elimination: evidence from the PKC theta knock-out mouse in vivo and in vitro. *J. Neurosci.* **24**, 3762-3769.
- Lichtman, J. W., Magrassi, L. and Purves, D.** (1987). Visualization of neuromuscular junctions over periods of several months in living mice. *J. Neurosci.* **7**, 1215-1222.
- Lingle, C. J. and Steinbach, J. H.** (1988). Neuromuscular blocking agents. *Int. Anesthesiol. Clin.* **26**, 288-301.
- Luscher, C., Xia, H., Beattie, E. C., Carroll, R. C., von Zastrow, M., Malenka, R. C. and Nicoll, R. A.** (1999). Role of AMPA receptor cycling in synaptic transmission and plasticity. *Neuron* **24**, 649-658.
- Madhavan, R., Zhao, X. T., Ruegg, M. A. and Peng, H. B.** (2005). Tyrosine phosphatase regulation of MuSK-dependent acetylcholine receptor clustering. *Mol. Cell. Neurosci.* **28**, 403-416.
- Malinow, R. and Malenka, R. C.** (2002). AMPA receptor trafficking and synaptic plasticity. *Annu. Rev. Neurosci.* **25**, 103-126.
- Mei, L. and Si, J.** (1995). Tyrosine phosphorylation and synapse formation at the neuromuscular junction. *Life Sci.* **57**, 1459-1466.
- Missias, A. C., Chu, G. C., Klocke, B. J., Sanes, J. R. and Merlie, J. P.** (1996). Maturation of the acetylcholine receptor in skeletal muscle: regulation of the AChR gamma-to-epsilon switch. *Dev. Biol.* **179**, 223-238.
- Moult, P. R., Schnabel, R., Kilpatrick, I. C., Bashir, Z. I. and Collingridge, G. L.** (2002). Tyrosine dephosphorylation underlies DHPG-induced LTD. *Neuropharmacology* **43**, 175-180.
- Moult, P. R., Gladding, C. M., Sanderson, T. M., Fitzjohn, S. M., Bashir, Z. I., Molnar, E. and Collingridge, G. L.** (2006). Tyrosine phosphatases regulate AMPA receptor trafficking during metabotropic glutamate receptor-mediated long-term depression. *J. Neurosci.* **26**, 2544-2554.
- Pahan, K., Sheikh, F. G., Namboodiri, A. M. and Singh, I.** (1998). Inhibitors of nitric-oxide synthase 1 and 2A differentially regulate the expression of inducible nitric-oxide synthase in rat astrocytes and macrophages. *J. Biol. Chem.* **273**, 12219-12226.
- Park, M., Penick, E. C., Edwards, J. G., Kauer, J. A. and Ehlers, M. D.** (2004). Recycling endosomes supply AMPA receptors for LTP. *Science* **305**, 1972-1975.
- Raymond, L. A., Blackstone, C. D. and Huganir, R. L.** (1993). Phosphorylation and modulation of recombinant GluR6 glutamate receptors by cAMP-dependent protein kinase. *Nature* **361**, 637-641.
- Raymond, L. A., Tingley, W. G., Blackstone, C. D., Roche, K. W. and Huganir, R. L.** (1994). Glutamate receptor modulation by protein phosphorylation. *J. Physiol. Paris* **88**, 181-192.
- Roche, K. W., Tingley, W. G. and Huganir, R. L.** (1994). Glutamate receptor phosphorylation and synaptic plasticity. *Curr. Opin. Neurobiol.* **4**, 383-388.
- Rotzler, S. and Brenner, H. R.** (1990). Metabolic stabilization of acetylcholine receptors in vertebrate neuromuscular junction by muscle activity. *J. Cell Biol.* **111**, 655-661.
- Rotzler, S., Schramek, H. and Brenner, H. R.** (1991). Metabolic stabilization of endplate acetylcholine receptors regulated by Ca²⁺ influx associated with muscle activity. *Nature* **349**, 337-339.
- Turney, S. G., Culican, S. M. and Lichtman, J. W.** (1996). A quantitative fluorescence-imaging technique for studying acetylcholine receptor turnover at neuromuscular junctions in living animals. *J. Neurosci. Methods* **64**, 199-208.
- van Mier, P. and Lichtman, J. W.** (1994). Regenerating muscle fibers induce directional sprouting from nearby nerve terminals: studies in living mice. *J. Neurosci.* **14**, 5672-5686.
- Wallace, B. G.** (1994). Staurosporine inhibits agrin-induced acetylcholine receptor phosphorylation and aggregation. *J. Cell Biol.* **125**, 661-668.
- Wallace, B. G., Qu, Z. and Huganir, R. L.** (1991). Agrin induces phosphorylation of the nicotinic acetylcholine receptor. *Neuron* **6**, 869-878.
- Yumoto, N., Wakatsuki, S. and Sehara-Fujisawa, A.** (2005). The acetylcholine receptor gamma-to-epsilon switch occurs in individual endplates. *Biochem. Biophys. Res. Commun.* **331**, 1522-1527.